

Automated Calculation of T2* mapping for MR Images with Application of Certainty Criterion for Enhanced Display

O. Adeyanju¹, E. Heirberg², and J. Sjögren³

¹Biomedical Engineering, Northwestern University, Chicago, Illinois, United States, ²Clinical Physiology, Lund University, Lund, Sweden, ³Engineering, Medviso AB, Lund, Sweden

Introduction

T2* mapping is a widely used method of relaxometry measurement with broad applications for BOLD functional MRI measurement¹, the quantification of superparamagnetic iron oxide particles², and other clinical uses (e.g. patient diseases that induce iron-overloading³). Segment (Medviso, AB) contains a new module that supports the automatic quantification and generation of T2* maps, circumventing the necessity of user-generated code and lengthy curve fitting processes. The purpose of this study was to assess and validate the Segment Software's T2* mapping measurements as well as its goodness of fit criterion, termed the certainty map. Segment is freely available for research purposes at <http://segment.heirberg.se>.

Methods

Data Acquisition We used a 1.5T clinical MRI scanner (Magnetom Espree™, Siemens Medical Solutions). A conventional mGRE sequence with 12 echoes was used for T2* images. FOV: 150mm Matrix: 192x192 Acquisition Time: 1:12 BW: 590 TR/TE: 375/3.27, Echo Spacing: 4.38ms. Flip Angle: 40° FA. **Phantoms:** Six phantoms were constructed with 2% agar and H₂O with YAS-SPIO microspheres (10% SPIO by mass, 38-45µm in diameter). Phantoms were prepared with the following concentrations: 0.04, 0.08, 0.12, 1, 3, 5, 10mg/mL. Phantoms were placed in a water bath with the same position between scans for an equivalent field shim. **Data Analysis** Regions of interest (ROI) were drawn over phantom locations in the T2* maps, and the mean T2* value in the ROI was calculated and used for comparison. ROIs were drawn from the original images and used for "ROI-averaged T2*map" (not pixel-by-pixel) calculations. **Segment algorithm:** T2* was calculated from fitting the phantom data with Equation 1 below, where S0 represents the calculated coefficient. Thereafter, Segment calculates an error map according to Equation 2 below where M0 represents the intensity of the image.

$$S0 \times e^{-\left(\frac{1}{T2^*} \times time\right)} \quad (\text{Equation 1}) \quad \text{Emap} = \frac{(M0 - S0 \times e^{-\left(\frac{1}{T2^*} \times time\right)})}{M0} \quad (\text{Equation 2})$$

Segment uses the error map to form a corresponding certainty map, C_{map}, where the pixels with the largest errors have been discarded. Segment then utilizes the certainty map to perform a normalized averaging on the T2* map for smoothing.

Comparison: Segment calculations were compared with standard linear least squares fitting computed without the use of certainty criteria. Pearson correlation coefficients with corresponding P values were calculated to assess the linear relationship between the T2* maps and both the ROI-averaged T2* maps as well as the concentrations of microspheres in the phantoms, with the assumption that a higher concentration of microsphere would result in a decreased T2*.

Results

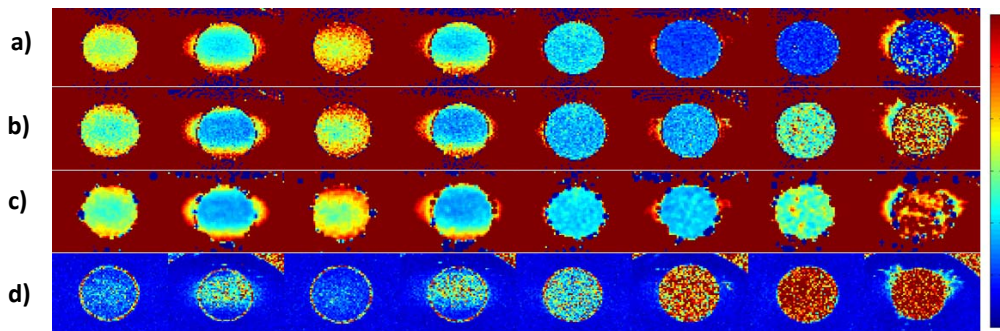


Figure 1 Maps for a) Standard T2* calculations, b) Segment's T2*, c) Segment with smoothing and d) the Error map.

Concentrations of microspheres going across: 0.04, 0.08, 0.12, 1, 3, 5, 10 mg/mL

Note that the T2* value generally decreases going across where the color map values range from 0 (cool/blue) to 60 (warm/red)

Table 1: Mean T2* Values for Different Calculation Methods at Various Concentrations

Mean T2* Values	Concentrations							
	0	0.04	0.08	0.12	1	3	5	10
Standard T2*	34.687	27.8279	40.7808	25.9888	20.5619	11.1436	9.6483	11.806
Segment T2*	31.2598	22.454	37.061	21.6729	20.1661	19.1389	29.7111	62.133
Segment (smoothed) T2*	31.4049	23.2769	37.3379	22.1737	20.5977	18.8332	28.4194	62.3281
Certainty Map Error (%)	13.7337	23.0576	10.9425	23.5237	26.9495	57.7382	71.1752	74.1673
ROI-averaged T2*	44.843	41.841	52.2486	23.31	20.202	10.9529	9.2421	6.7159

Correlation Coefficient (r)			
All Data			
	Concentration	ROI-averaged	StandardT2*
StandardT2*	-0.681 (P ~ 0.136)	0.974 (P ~ 0.001)	1 (P = 0)
SegmentT2*	0.779 (P ~ 0.068)	-0.078 (P ~ 0.883)	-0.0723 (P ~ 0.8917)
SegmentT2* (smoothed)	0.7622 (P ~ 0.078)	-0.0604 (P ~ 0.91)	-0.0483 (P ~ 0.892)
ROI-averaged values	-0.661 (P ~ 0.1526)	1 (P=0)	0.9736 (P ~ 0.001)

Correlation Coefficient (r)			
Data with <30% Error			
	Concentration	ROI-averaged	StandardT2*
StandardT2*	-0.734 (P ~ 0.4752)	0.9835 (P ~ 0.1159)	1 (P = 0)
SegmentT2*	-0.5994 (P ~ 0.5908)	1 (P ~ 0.0003)	0.9836 (P ~ 0.1156)
SegmentT2* (smoothed)	-0.6031 (P ~ 0.5878)	1 (P ~ 0.0033)	0.9844 (P ~ 0.1156)
ROI-averaged values	-0.599 (P ~ 0.5911)	1 (P=0)	0.9835 (P ~ 0.1156)

Discussion

The Segment T2* calculations had a higher correlation with the concentration and ROI-averaged measurements of T2* when the mean error value was less than 25% error. The two-sample t test comparing the mean Segment T2* values with the mean Standard T2* values failed to reject the null hypothesis with a P value of 0.191 indicating the two measurements are not statistically significantly different from one another.

Conclusion

Segment significantly improved the time of acquisition of T2* maps (approximately 10-fold) compared with generation and application of code using Matlab software. However, the accuracy of values is significantly related to the error depicted in the k map error estimate. This suggests that the use of Segment's T2* mapping module would be useful for the quick generation of T2* maps; however it should be in conjunction with an exclusion criteria where the Error map value must be less than or equal to 25. It is possible that the range of concentrations may also be restricted for improved measurements.

References

1. A. C. Schulte, O. Speck, C. Oesterle et al., *Magn Reson Med* **45** (5), 811 (2001).
2. R. Kuhlper, H. Dahnke, L. Matuszewski et al., *Radiology* **245** (2), 449 (2007).
3. A. Inati, K. M. Musallam, J. C. Wood et al., *Eur J Haematol* (2009).
4. E. Heirberg, M. Ugander, H. Engblom et al., *Radiology* **246** (2), 581 (2008).